

Research Article

Zero and Nonzero Mass Flux Effects of Bioconvective Viscoelastic Nanofluid over a 3D Riga Surface with the Swimming of Gyrotactic Microorganisms

T. S. Karthik,¹ K. Loganathan ,² A. N. Shankar,³ M. Jemimah Carmichael,⁴ Anand Mohan,⁵ Mohammed K. A. Kaabar ,⁶ and Safak Kayikci ⁷

¹Department of Electronics and Communication Engineering, Aditya College of Engineering and Technology, Surampalem, 533 437 Andhra Pradesh, India

²Research and Development Wing, Live4Research, Tiruppur, 638 106 Tamilnadu, India

³Department of HSE Civil Engineering, University of Petroleum Energy Studies, Uttarakhand, India

⁴Department of Civil Engineering, Vignans' Lara Institute of Technology and Science, Guntur, Andhra Pradesh, India

⁵Department of Physics, LN Mithila University, Darbhanga, Bihar, India

⁶Jabalia Camp, UNWRA Palestinian Refugee Camp, Gaza Strip Jabalya, State of Palestine

⁷Department of Computer Engineering, Bolu Abant Izzet Baysal University, Bolu, Turkey

Correspondence should be addressed to K. Loganathan; loganathankaruppusamy304@gmail.com and Mohammed K. A. Kaabar; mohammed.kaabar@wsu.edu

Received 25 March 2021; Revised 15 May 2021; Accepted 11 June 2021; Published 16 July 2021

Academic Editor: Mustafa Inc

Copyright © 2021 T. S. Karthik et al. This is an open access article distributed under the Creative Commons Attribution License, which permits unrestricted use, distribution, and reproduction in any medium, provided the original work is properly cited.

This work addresses 3D bioconvective viscoelastic nanofluid flow across a heated Riga surface with nonlinear radiation, swimming microorganisms, and nanoparticles. The nanoparticles are tested with zero (passive) and nonzero (active) mass flux states along with the effect of thermophoresis and Brownian motion. The physical system is visualized via high linearity PDE systems and nondimensionalized to high linearity ordinary differential systems. The converted ordinary differential systems are solved with the aid of the homotopy analytic method (HAM). Several valuable and appropriate characteristics of related profiles are presented graphically and discussed in detail. Results of interest such as the modified Hartmann number, mixed convection parameter, bioconvection Rayleigh number, and Brownian motion parameter are discussed in terms of various profiles. The numerical coding is validated with earlier reports, and excellent agreement is observed. The microorganisms are utilized to improve the thermal conductivity of nanofluid, and this mechanism has more utilization in the oil refinery process.

1. Introduction

“Bioconvection” is known to be the convective movement within sight of swimming microorganisms. In this convective mode, the cells with bottom-heavy cells tend to swim at an angle to vertical, and this process is known as gyrotactic [1]. Therefore, the gyrotactic microorganisms are stable in the upper layer of the fluid, and consequently, stratification of the top-heavy fluid layer will become unbalanced. Thus, the system, which consists of a gyrotactic microorganism, induces one of the exciting characters in heat transfer that is “stability.” The reason is that nano-

fluids that have higher stability tend to improve the thermal efficiency of the heat exchanger (any energy systems). Hosseinzadeh et al. [2] examined the gyrotactic microorganism influence over a cylindrical surface with cross fluid flow. Mogharrebi et al. [3] present the MHD nanofluid flow towards a rotating cone with motile oxytactic microorganisms. Nowadays, the research on nanofluid through a Riga plate becomes an exciting area of research. For instance, mixed convective nanofluid flowed a Riga plate is studied numerically and analytically in [4]. It is shown that the desired size of the nanoparticle influences the skin friction coefficient. Ahmad et al. [5] studied the

role of nanofluid past a heated vertical Riga plate numerically. Influence on viscous dissipation and thermal radiation of nanofluid flow between the Riga plate is explored numerically [6]. They have used carbon nanotubes as the nanoparticle, and it is shown that by varying the radiation parameter, the local heat transfer rate elevates. The application of the Cattaneo-Christov approach heat generation and absorption for the second-grade fluid that passed through the Riga plate is presented numerically [7]. In line with the application of the Riga plate, the stagnation flow on the vacillating Riga plate is studied numerically [8]. The variable thicked Riga plate for melting heat transfer application is explored numerically, and it is reported that for higher values of modified Hartmann number, the velocity profile distribution increases [9]. Recently, several research papers have been devoted to the study of nanofluid and their applications in practical situations [10–13].

Further, the study on heat transfer characteristics of nanofluid is widely studied. For instance, viscoelastic fluid with Newtonian heating is numerically studied [14–17]. It is shown that $\text{Al}_2\text{O}_3/\text{water}$ nanofluid exhibits higher performance evaluation criteria. Besides, the study of viscoelastic nanofluid through the Riga plate is extensively studied. A nonuniform heat flux unsteady viscoelastic fluid that is unsteady is numerically investigated [18]. The viscoelastic nanofluid over an unsteady surface that is stretchable is evaluated numerically [19]. Also, the magnetic field effect on the Maxwell viscoelastic nanofluid over a plate that is moving at a uniform velocity is numerically assessed [20]. The temperature and velocity relaxation time influencing the heat transfer rate of the nanofluid are concluded by them. Besides that, the nonlinear effects on the MHD stagnation flow of viscoelastic nanofluid are explored numerically [21]. The Homotopy Analysis Method (HAM) is employed by Hayat et al. [22] to solve the 3D flow of a viscoelastic nanofluid over a stretching surface. The same research group extended their work towards the viscoelastic model for various applications [23–25]. A slew of researchers studies the gyrotactic microorganism impact. For example, mixed convection of nanofluid containing third-grade nanomaterial containing gyrotactic microorganisms is figured out numerically [26]. Walters B nanofluid with the incorporation of gyrotactic microorganisms is evaluated numerically [27]. Acharya et al. [28] reported the effects of solar radiation bioconvection nanofluid with gyrotactic microorganisms. The suspension of microorganisms induced with the effect of the magnetic field is reported [29, 30]. Also, numerous researches on gyrotactic microorganisms are studied and explored [30–35]. Analysis of active and passive controls with the chemical reaction of nanofluid is analyzed [36]. Using the homotopy perturbation method, unsteady nanofluid with active and passive controls is developed by Acharya et al. [37]. Over a bent surface, the active-passive control of dihydrogen monoxide nanofluid is explored numerically [38]. These controls are studied in various nanofluids with diverse applications [39–44].

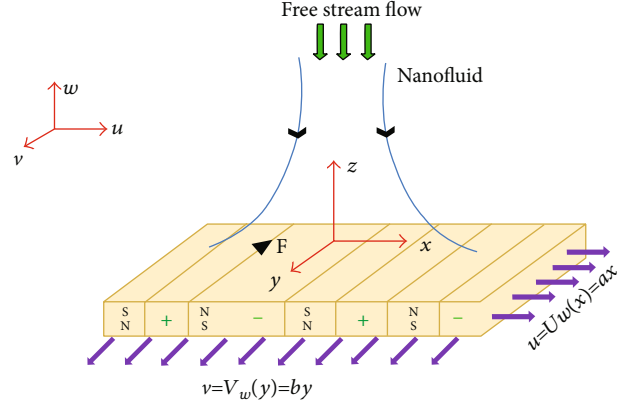


FIGURE 1: Geometry of flow problem.

By considering the earlier reports, it is concluded that no studies were found to analyze the bioconvection of viscoelastic nanofluid on a 3D Riga surface with a comparison of active and passive control. The present study explores the 3D viscoelastic nanofluid flow across the heated Riga surface with nonlinear radiation and heat generation/absorption effects. The effects of several parameters are compared with the active and passive control model of nanoparticles. The homotopy analytic method [45–51] is employed to study the present nonlinear ODE systems. The results are discussed in terms of various profiles. The numerical coding of the present study is validated with earlier reports. The relevant research is applied to multiple engineering streams like bioengineering, chemical, nuclear, thermal, and mechanical.

2. Problem Development

We have considered bioconvective viscoelastic nanofluid flow with $u_w = ax$ in the x direction $v_w = by$ in the y direction over a 3D Riga surface with gyrotactic microorganisms swimming. The surface is expanding in all three directions, namely, x , y , and z . It is assumed that nanoparticles do not influence the swimming microorganism; also, the nanoparticles are assumed to be stable in the fluid layer. Also, the nanoparticles have no effect on the velocity and temperature of the swimming microorganisms. The geometrical configuration is shown in Figure 1. By considering the above assumptions, the governing equations are described below [42]:

$$\begin{aligned} \frac{\partial u}{\partial x} + \frac{\partial v}{\partial y} + \frac{\partial w}{\partial z} &= 0, \\ u \frac{\partial u}{\partial x} + v \frac{\partial u}{\partial y} + w \frac{\partial u}{\partial z} &= v \frac{\partial^2 u}{\partial z^2} \\ &- \alpha \left[u \frac{\partial^3 u}{\partial x \partial z^2} + w \frac{\partial^3 u}{\partial z^3} - \frac{\partial u}{\partial x} \frac{\partial^2 u}{\partial z^2} - \frac{\partial u}{\partial z} \frac{\partial^2 u}{\partial z^2} - 2 \frac{\partial u}{\partial z} \frac{\partial^2 u}{\partial x \partial z} - 2 \frac{\partial w}{\partial z} \frac{\partial^2 u}{\partial z^2} \right] \\ &+ \frac{1}{\rho_f} \left[(1 - C_\infty) \rho_f \beta g (T - T_\infty) - (\rho_p - \rho_f) g (C - C_\infty) \right. \\ &\left. - (n - n_\infty) g \omega (\rho_m - \rho_f) \right] + \frac{\pi j_0 M_0 \exp(-(\pi/e)z)}{8\rho}, \end{aligned}$$

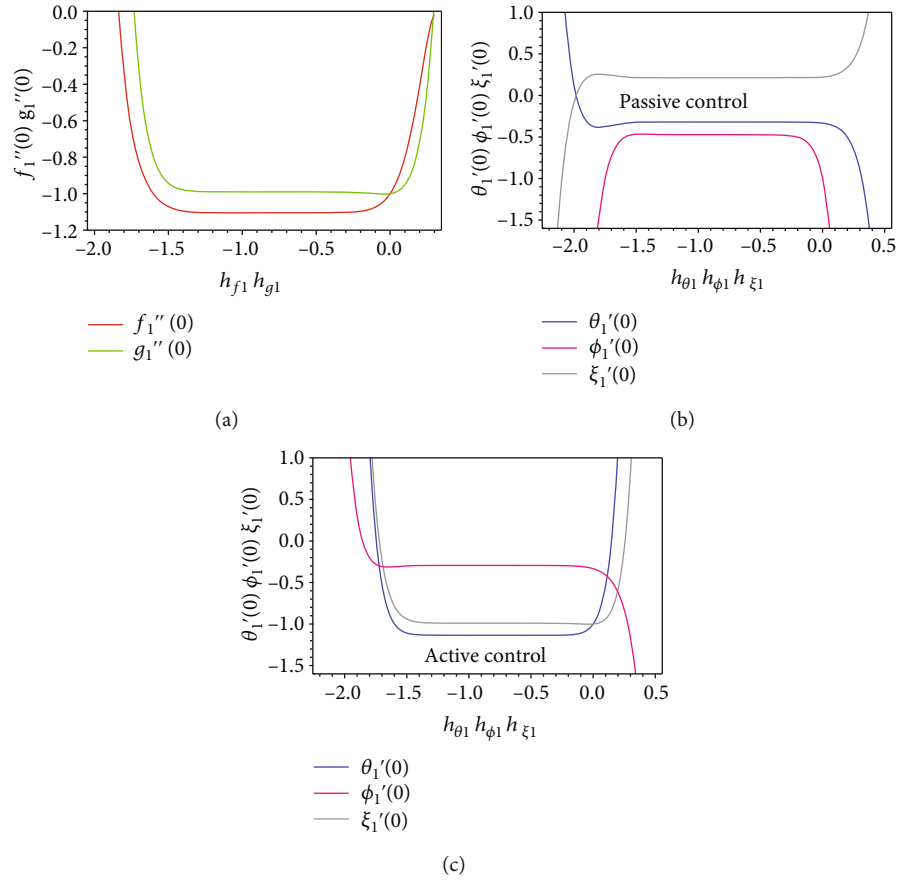


FIGURE 2: Convergence plots of the HAM solution.

$$u \frac{\partial v}{\partial x} + v \frac{\partial v}{\partial y} + w \frac{\partial v}{\partial z} = v \frac{\partial^2 v}{\partial z^2} - \alpha \left[v \frac{\partial^3 v}{\partial y \partial z^2} + w \frac{\partial^3 v}{\partial z^3} - \frac{\partial v \partial^2 v}{\partial y \partial z^2} - \frac{\partial v \partial^2 w}{\partial z \partial z^2} - 2 \frac{\partial v \partial^2 v}{\partial z \partial y \partial z} - 2 \frac{\partial w \partial^2 v}{\partial z \partial z^2} \right],$$

$$\rho c_p \left[u \frac{\partial T}{\partial x} + v \frac{\partial T}{\partial y} + w \frac{\partial T}{\partial z} \right] = k \frac{\partial^2 T}{\partial z^2} + \tau \left[D_B \frac{\partial C \partial T}{\partial z \partial z} + \frac{D_T}{T_\infty} \left(\frac{\partial T}{\partial z} \right)^2 \right] - \frac{\partial q_r}{\partial z} + \frac{Q_0}{\rho c_p} (T - T_\infty),$$

$$u \frac{\partial C}{\partial x} + v \frac{\partial C}{\partial y} + w \frac{\partial C}{\partial z} = D_B \frac{\partial^2 C}{\partial z^2} + \frac{D_T}{T_\infty} \frac{\partial^2 T}{\partial z^2} - K_m (C - C_\infty),$$

$$u \frac{\partial N}{\partial x} + v \frac{\partial N}{\partial y} + w \frac{\partial N}{\partial z} - D_N \left(\frac{\partial^2 N}{\partial z^2} \right) = - \frac{dW_c}{(C_w - C_\infty)} \left[\frac{\partial}{\partial z} \left(N \frac{\partial C}{\partial z} \right) \right].$$

(1)

 TABLE 1: Order of approximation for $-f_1''(0)$ and $-g_1''(0)$.

Order of approximation	$-f_1''(0)$		$-g_1''(0)$	
	Active	Passive	Active	Passive
1	1.1062	1.0642	1.0062	1.0437
5	1.1410	1.0997	0.9900	1.0467
10	1.1409	1.1019	0.9892	1.0456
15	1.1408	1.1023	0.9892	1.0455
20	1.1408	1.1025	0.9892	1.0455
25	1.1408	1.1025	0.9892	1.0454
30	1.1408	1.1025	0.9892	1.0454
35	1.1408	1.1025	0.9892	1.0454

With boundary conditions

$$\begin{aligned} u(x, y, 0) &= ax, v(x, y, 0) = by, w(x, y, 0) = 0, -k \frac{\partial T}{\partial z}(x, y, 0) \\ &= h_f [T_f(x, y, 0) - T(x, y, 0)], C(x, y, 0) \\ &= C_w(x), (AC), D_B \frac{\partial C}{\partial z}(x, y, 0) + \frac{D_T}{T_\infty} \frac{\partial T}{\partial z}(x, y, 0) \\ &= 0, (PC) N(x, y, 0) = N_w(x), \end{aligned}$$

(2)

$$\begin{aligned}
u(x, y, \infty) = 0, v(x, y, \infty) = 0, \frac{\partial u}{\partial z}(x, y, \infty) = 0, \frac{\partial v}{\partial z}(x, y, \infty) \\
= 0, T(x, y, \infty) = T_\infty, C(x, y, \infty) = C_\infty, N(x, y, \infty) \\
= N_\infty.
\end{aligned} \tag{3}$$

Now, we state the nondimensional similarity variables below:

$$\begin{aligned}
f_1'(\eta) &= \frac{u}{ax}, \eta = \left(\frac{a}{v}\right)^{0.5} z, g_1'(\eta) = \frac{v}{ay}, [f_1(\eta) + g_1(\eta)] \\
&= -\frac{w}{(av)^{0.5}}, \theta(\eta) = \frac{T - T_\infty}{T_f - T_\infty}, \phi(\eta) \\
&= \frac{C - C_\infty}{C_w - C_\infty} \text{ (AC)}, \phi(\eta) = \frac{C - C_\infty}{C_\infty} \text{ (PC)}, \xi(\eta) \\
&= \frac{N - N_\infty}{N_w - N_\infty}.
\end{aligned} \tag{4}$$

Using the transformations in Equation (1), we get

$$\begin{aligned}
f_1''' - (f_1')^2 + (f_1 + g_1)f_1'' + \gamma \left[(f_1 + g_1)f_1^{iv} + (f_1'' - g_1'')f_1'' - 2(f_1' + g_1')f_1''' \right] \\
+ (\lambda\theta_1 - \text{Nr}\phi_1 - \text{Rb}\xi_1) + Qe^{-d_1\eta} = 0, \\
g_1''' - (g_1')^2 + (f_1 + g_1)g_1'' + \gamma \left[(f_1 + g_1)g_1^{iv} + (f_1'' - g_1'')g_1'' - 2(f_1' + g_1')g_1''' \right] = 0, \\
\frac{1}{\text{Pr}}\theta_1'' + \frac{\text{Rd}}{\text{Pr}}((\theta_1(\theta_w - 1) + 1))^2(3\theta_1'^2(\theta_w - 1) + (\theta_1(\theta_w - 1) + 1)\theta_1'') \\
+ (f_1 + g_1)\theta_1' + \text{Nb}\phi_1'\theta_1' + \text{Nt}(\theta_1')^2 + \text{Hg}\theta,
\end{aligned}$$

$$\phi_1'' + \text{Le}(f_1 + g_1)\phi_1' + \frac{\text{Nt}}{\text{Nb}}\theta_1'' - \text{LeCr}\phi_1 = 0,$$

$$\xi_1'' + \text{Lb}(f_1 + g_1)\xi_1' - P_e \left[\phi_1''(\xi_1 + \Omega) + \phi_1'\xi_1' \right] = 0. \tag{5}$$

Boundary condition (2) and (3) in expressions of $f_1, g_1, \theta_1, \phi_1,$ and ξ_1 is developed:

$$\begin{aligned}
f_1(0) = 0, g_1(0) = 0, f_1'(0) = 1, g_1'(0) = \epsilon, f_1'(\infty) = 0, g_1'(\infty) = 0, \\
f_1''(\infty) = 0, g_1''(\infty) = 0, \theta_1'(0) = -\text{Bi}(1 - \theta_1(0)), \theta_1(\infty) = 0, \\
\text{Nb}\phi_1' + \text{Nt}\theta_1' = 0, \phi_1(\infty) = 0 \text{ (PC)}, \\
\phi_1(0) = 1, \phi_1(\infty) = 0 \text{ (AC)}, \\
\xi_1(0) = 1, \xi_1(\infty) = 0.
\end{aligned} \tag{6}$$

TABLE 2: Order of approximation for $-\theta_1'(0), -\phi_1'(0),$ and $-\xi_1'(0).$

Order of approximation	$-\theta_1'(0)$		$-\phi_1'(0)$		$-\xi_1'(0)$	
	Active	Passive	Active	Passive	Active	Passive
1	0.3141	0.3241	0.975	—	0.917	0.6363
5	0.3010	0.3196	0.9274	—	0.8585	0.4737
10	0.3003	0.3193	0.9334	—	0.8653	0.4657
15	0.3002	0.3193	0.9336	—	0.8657	0.4645
20	0.3002	0.3193	0.9336	—	0.8657	0.4641
25	0.3002	0.3193	0.9336	—	0.8657	0.4641
30	0.3002	0.3193	0.9336	—	0.8657	0.4641
35	0.3002	0.3193	0.9336	—	0.8657	0.4641

TABLE 3: Comparison of $-f_1''(0)$ and $-g_1''(0)$ for various values of ϵ with limiting conditions $Q = d_1 = \lambda = \text{Nr} = \text{Rb} = 0.$

ϵ	$-f_1''(0)$		$-g_1''(0)$	
	Qayyum et al. [14]	Present	Qayyum et al. [14]	Present
0.0	1.000000	1.00000	0.000000	0.00000
0.1	1.020259	1.02026	0.066947	0.06685
0.2	1.039495	1.03950	0.148736	0.14874
0.3	1.057954	1.05795	0.243359	0.24336
0.4	1.075788	1.07579	0.349208	0.34921
0.5	1.093095	1.09309	0.465204	0.46521
0.6	1.109946	1.10995	0.590528	0.59053
0.7	1.126397	1.12640	0.724531	0.72453
0.8	1.142488	1.14249	0.866682	0.86668
0.9	1.158253	1.15825	1.016538	1.01654
1.0	1.173720	1.17371	1.173720	1.17371

The dimensionless variables are

$$\begin{aligned}
\gamma &= \frac{\alpha a}{v}, \epsilon = \frac{b}{a}, \text{Pr} = \frac{\rho c_p}{k}, \text{Bi} = \frac{h_f}{k} \sqrt{\frac{v}{a}}, \text{Nb} = \frac{\tau D_B}{v} C_\infty, \text{Nt} \\
&= \frac{\tau D_T}{v} (T_f - T_\infty), \text{Cr} = \frac{K_m}{a}, \text{Hg} = \frac{Q_0}{\rho c_p a}, Q = \frac{\pi j_0 M_0}{8a^3 x \rho}, \theta_w \\
&= \frac{T_w}{T_\infty}, \text{Lb} = \frac{v}{D_m}, \text{Pe} = \frac{dW_c}{D_m}, \lambda = \frac{\beta \omega (1 - C_\infty)(T_w - T_\infty)}{au_w}, \text{Nr} \\
&= \frac{(\rho_p - \rho_f)}{\beta \rho_f} \frac{(C_w - C_\infty)}{(T_f - T_\infty)}, \text{Rb} = \frac{\omega(N_w - N_\infty)(\rho_m - \rho_f)}{\beta \rho_f (1 - C_\infty)(T_f - T_\infty)}.
\end{aligned} \tag{7}$$

The nondimensional structure of surface drag force (C_{fx} & C_{fy}) and heat transfer rate (Nu), mass transfer rate (Sh),

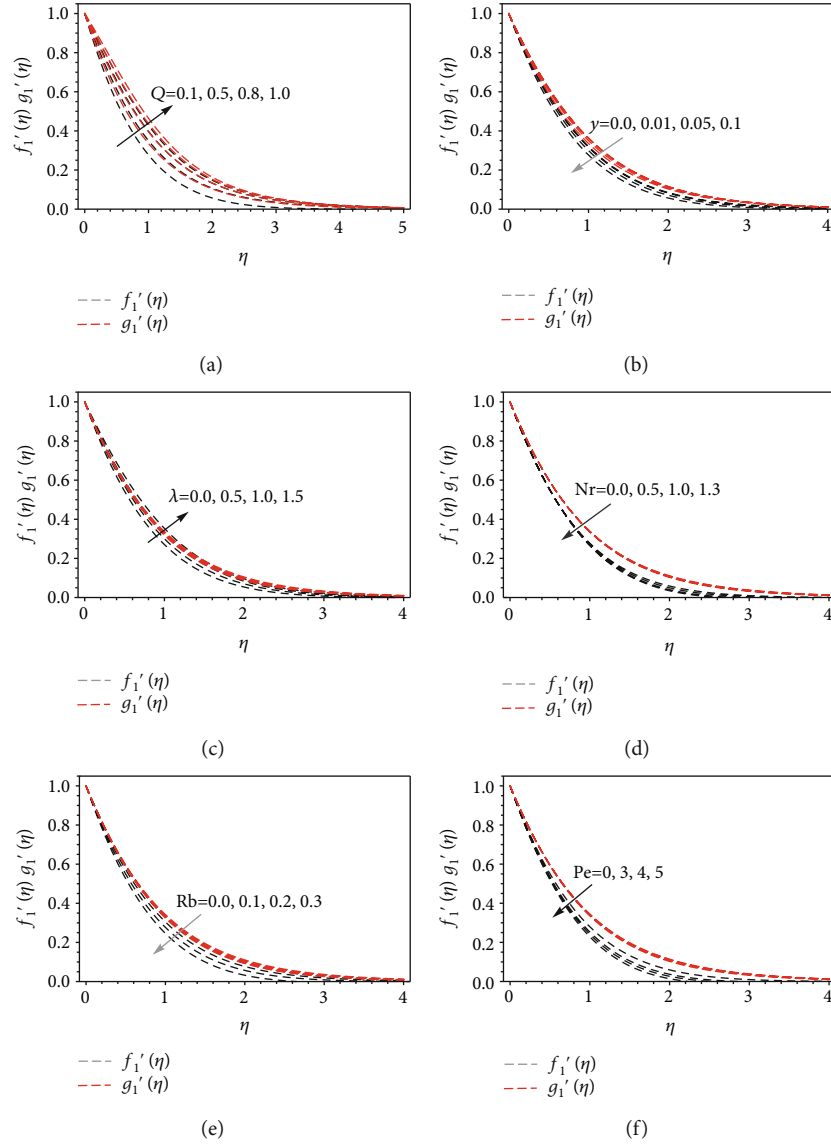


FIGURE 3: Velocity profile on x and y directions for various values of $Q, \gamma, \lambda, Nr, Rb,$ and Pe .

and microorganism (Nn) density number is stated as

$$C_{fx} Re^{0.5} = \left[f_1'' + \gamma \left\{ 2f_1' f_1'' - f_1''' (f_1 + g_1) + (f_1' + g_1') f_1'' \right\} \right]_{\eta=0},$$

$$C_{fy} Re^{0.5} = \left[g_1'' + \gamma \left\{ 2g_1' g_1'' - g_1''' (f_1 + g_1) + (f_1' + g_1') g_1'' \right\} \right]_{\eta=0},$$

$$Nu Re^{-0.5} = - \left[1 + \frac{4}{3} Rd(\theta_w)^3 \right]_{\eta=0},$$

$$Sh Re^{-0.5} = - \left[\phi_1' \right]_{\eta=0} \text{ (AC)},$$

$$Sh Re^{-0.5} = \left[\frac{Nt}{Nb} \theta_1' \right]_{\eta=0} \text{ (PC)},$$

$$Nn Re^{-0.5} = - \left[\xi_1' \right]_{\eta=0}.$$

(8)

3. Solution Approach: Homotopy Analysis Method (HAM)

The primary assumptions of the homotopy analytic method are stated as follows:

$$\begin{aligned} f_{1(0)} &= 1 - \exp(-\eta), g_{1(0)} = \epsilon * 1 - \exp(-\eta), \theta_{1(0)} \\ &= \frac{Bi * \exp(-\eta)}{1 + Bi}, \phi_{1(0)} = \exp(-\eta) \text{ (AC)}, \phi_{1(0)} \\ &= - \left(\frac{Nt}{Nb} \right) * \frac{Bi * \exp(-\eta)}{1 + Bi} \text{ (PC)}, \xi_{1(0)} = \exp(-\eta). \end{aligned} \tag{9}$$

The auxiliary linear operators $L_{f_1}, L_{g_1}, L_{\theta_1}, L_{\phi_1},$ and L_{ξ_1}

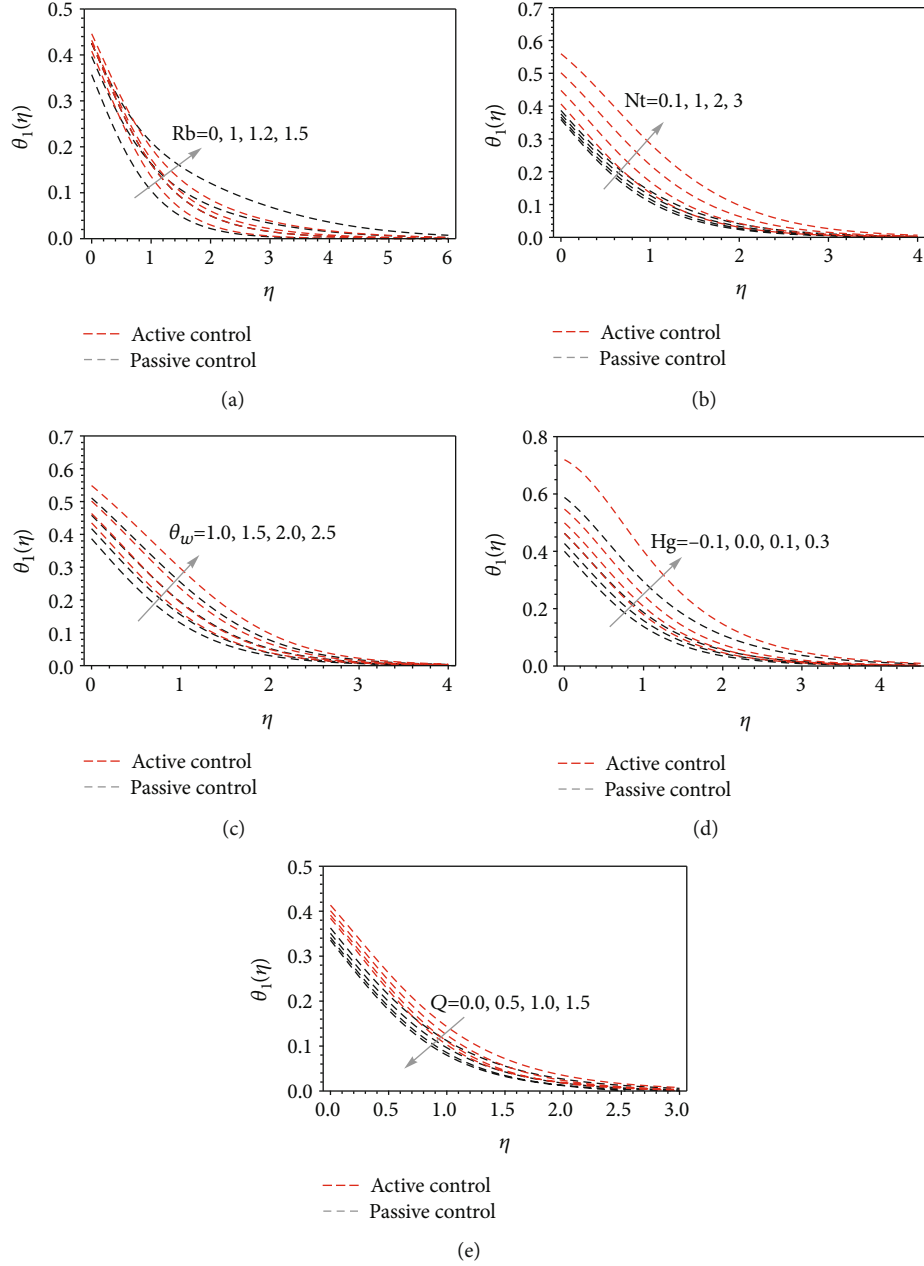


FIGURE 4: Temperature profiles for various values of Rb, Nt, Hg, θ_w , and Q.

are derived as

$$\begin{aligned}
 L_{f_1} &= f_1'''(\eta) - f_1'(\eta), L_{g_1} = g_1'''(\eta) - g_1'(\eta), L_{\theta_1} \\
 &= \theta_1''(\eta) - \theta_1(\eta), L_{\phi_1} = \phi_1''(\eta) - \phi_1(\eta), L_{\xi_1} \\
 &= \xi_1''(\eta) - \xi_1(\eta).
 \end{aligned} \quad (10)$$

The above linear operators satisfying

$$\begin{aligned}
 L_{f_1}[S_1 + S_2e^{\eta} + S_3e^{-\eta}] &= 0, L_{g_1}[S_4 + S_5e^{\eta} + S_6e^{-\eta}] \\
 &= 0, L_{\theta_1}[S_7e^{\eta} + S_8e^{-\eta}] = 0, L_{\phi_1}[S_9e^{\eta} + S_{10}e^{-\eta}] \\
 &= 0, L_{\xi_1}[S_{11}e^{\eta} + S_{12}e^{-\eta}] = 0.
 \end{aligned} \quad (11)$$

The appropriate solutions $[f_{1m}^*, g_{1m}^*, \theta_{1m}^*, \phi_{1m}^*, \xi_{1m}^*]$ are

$$\begin{aligned}
 f_{1m}(\eta) &= f_{1m}^*(\eta) + S_1 + S_2e^{\eta} + S_3e^{-\eta}, \\
 g_{1m}(\eta) &= g_{1m}^*(\eta) + S_4 + S_5e^{\eta} + S_6e^{-\eta}, \\
 \theta_{1m}(\eta) &= \theta_{1m}^*(\eta) + S_7e^{\eta} + S_8e^{-\eta}, \\
 \phi_{1m}(\eta) &= \phi_{1m}^*(\eta) + S_9e^{\eta} + S_{10}e^{-\eta}, \\
 \xi_{1m}(\eta) &= \xi_{1m}^*(\eta) + S_{11}e^{\eta} + S_{12}e^{-\eta},
 \end{aligned} \quad (12)$$

where $S_j (j = 1 - 12)$ denote the arbitrary conditions.

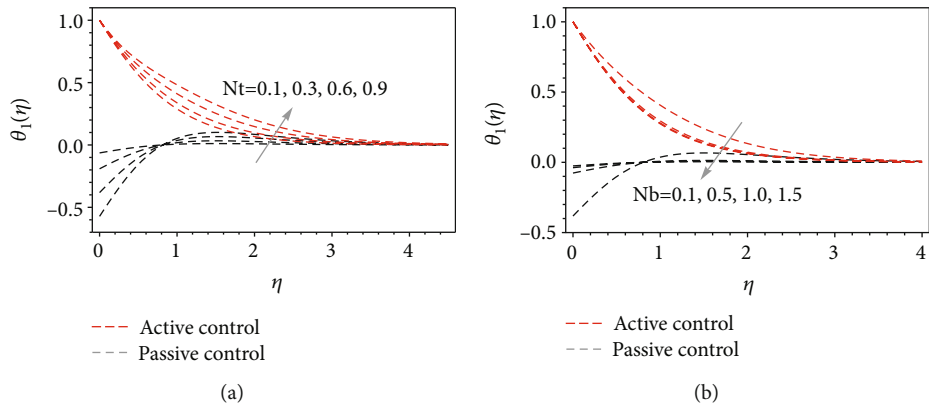


FIGURE 5: Nanoparticle concentration profile for various values of Nt and Nb .

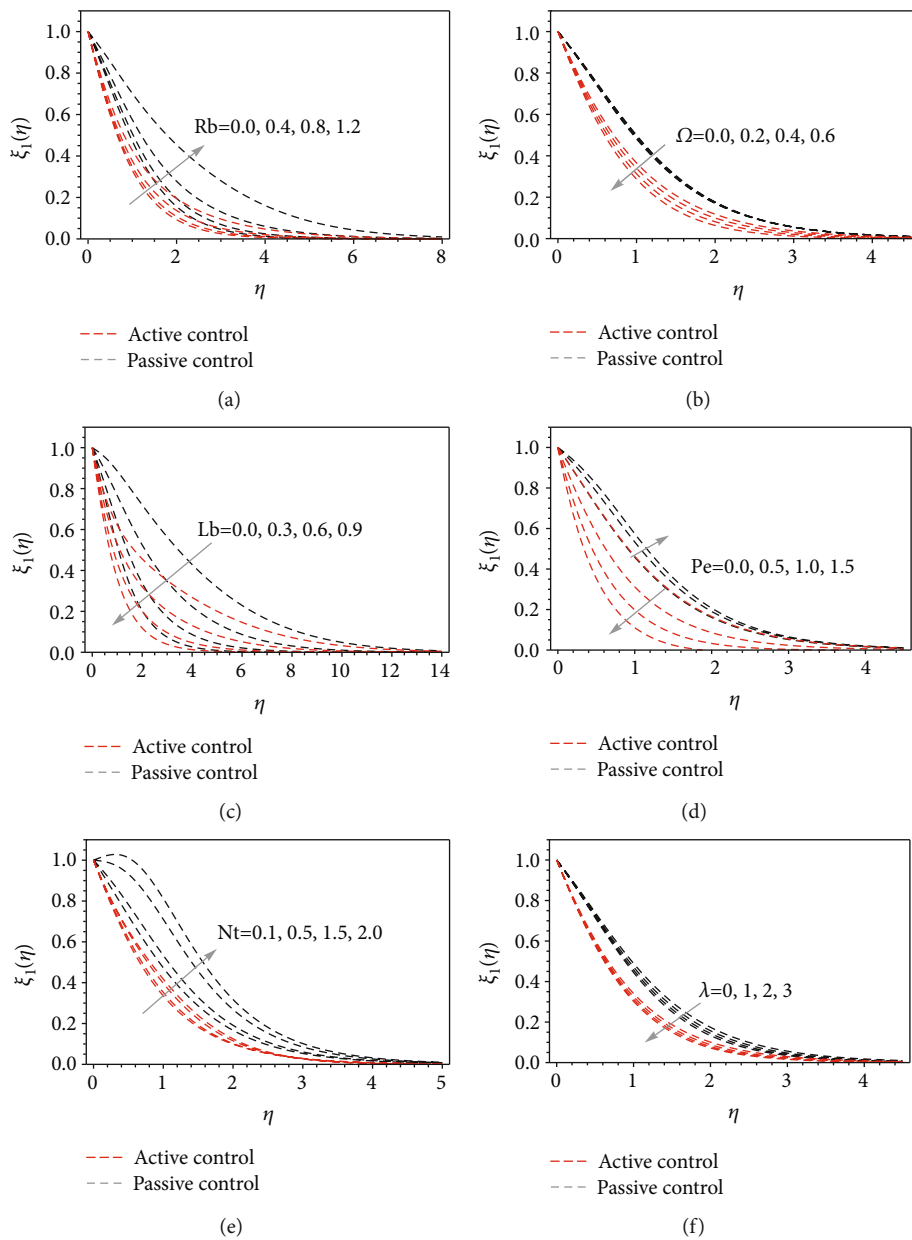


FIGURE 6: Motile density profile for various values of Rb , Ω , Lb , Pe , Nt , and λ .

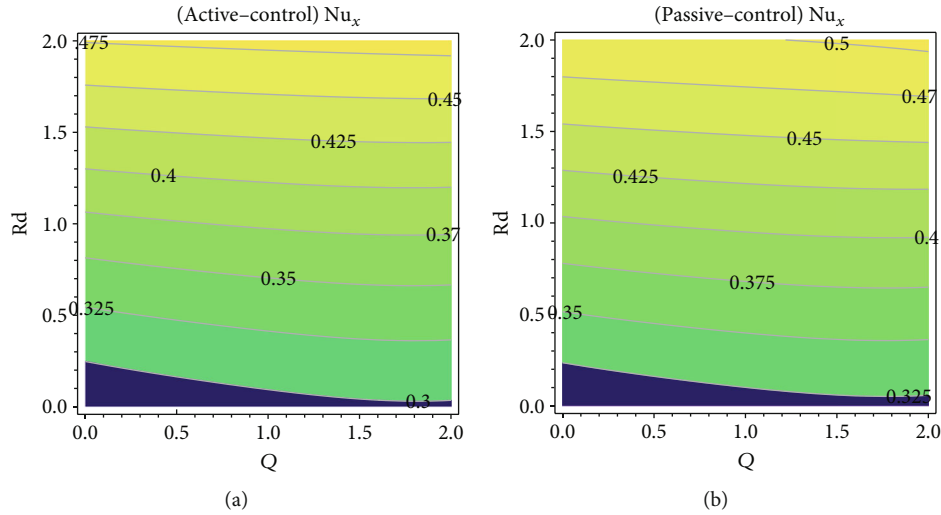


FIGURE 7: The effect of Nusselt number for combined parameters Rd and Q .

4. Convergence Analysis

To analyze the convergence of the numerical code, the convergence analysis is carried out for the value of \mathbf{h} . The variable \mathbf{h} has control over the convergence and divergence of the numerical code, and it is shown in Figure 2. In the case of active and passive control, the values of $\mathbf{h}_f, \mathbf{h}_g, \mathbf{h}_\phi, \mathbf{h}_\theta, \mathbf{h}_\xi$ in the range of $-2.0 \leq \mathbf{h}_f, \mathbf{h}_g, \mathbf{h}_\phi, \mathbf{h}_\theta, \mathbf{h}_\xi \leq 0.5$. For the convergence study in the direction of x and y axes, the value of $\mathbf{h}_f, \mathbf{h}_g$ is in the range of -2.0 to 0.5, respectively. The order of approximation is shown in Tables 1 and 2. Table 3 reports that the value of $f'_1(0)$ and $g'_1(0)$ is compared with earlier results with Qayyum et al. [14].

5. Results and Discussions

In this work, viscoelastic nanofluid past a stretching 3D Riga surface with gyrotactic microorganisms is explored numerically. The governing parameters such as velocity (f_1, g_1) parameters, temperature (θ_1) parameter, ξ , modified Hartmann number (Q), viscoelastic parameter (γ), mixed convection parameter (λ), buoyancy ratio parameter (Nr), bioconvection Rayleigh number (Rb), bioconvection Peclet number (Pe), heat generation/absorption parameter (Hg), thermophoresis parameter (Nt), and microorganism concentration difference parameter (Ω) are studied.

Figure 3(a) describes the impact of Q (modified Hartmann's number) on the velocity profile. It is observed that with an increase in Q , velocity profiles decrease in both directions (x, y). This is due to the increase in Q leading to an increase in Lorentz force and consequently velocity profile decreases. In Figure 3(b), it is noticed that as the viscoelastic parameter (γ) increases, the velocity profile decreases. In general, tensile stress is generated by viscoelasticity of the fluid. This stress opposes the fluid motion, and finally, the velocities of x and y directions are decays when the values of γ are improved. The increase in velocity profile is noted in

Figure 3(c) with an enhancement in the mixed convection parameter (λ). By definition, λ is the ratio between the buoyancy force and the viscous force. Figure 3(d) reveals that an increase in buoyancy ratio parameter velocity profile decreases. In this work, the thermal and concentration forces are considered, and those forces provide smaller resistance consequently due to this reason that the velocity profile decreases. Also, it is observed in Figure 3(e) that the extending values of bioconvection Rayleigh number have a tendency to diminish the velocity profile. In Figure 3(f), it is noted that an increase in the bioconvection Peclet number produces the diminishing performance in the swimming speed of microorganisms that cause a decreasing trend in the velocity profile.

From Figure 4(a), it is evident that the increase in temperature profile increases with an increase in bioconvection Rayleigh number (Rb). In fact, for larger values of Rb , boundary layer thickness increases which increases the buoyancy forces; subsequently, temperature profile increases for both the cases of active and passive controls. The impact of temperature profile with regard to the thermophoresis parameter Nt is discussed in Figure 4(b). With an increase in the thermophoresis parameter, Nt temperature profile is increased. With an increase in Nt , more nanoparticles shifted to the colder place from the hotter one, so the temperature profile increases. An increase in temperature ratio parameter θ_w increases the temperature profile as observed in Figure 4(c). The ratio of temperature at the surface (T_w) to the temperature at free stream (T_∞) is mathematically defined as $\theta_w = T_w/T_\infty$. For nonlinear radiation, the value of θ_w must be higher than 1. Moreover, an increasing trend found in the temperature along the surface is noted for larger θ_w values. Consequently, thermal boundary and associated layer thickness improve. The effect of the heat generation/absorption parameter, Hg on the temperature profile, is proclaimed in Figure 4(d). As we increase Hg , more movement between the nanoparticles is reported; therefore, the temperature profile increases. The slowing moment of the liquid flow due to

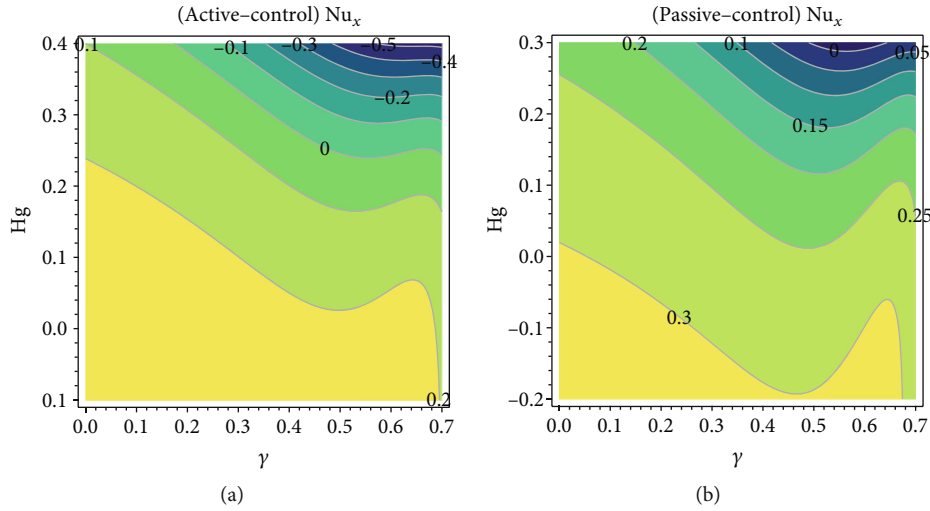


FIGURE 8: The effect of Nusselt number for combined parameters Hg and γ .

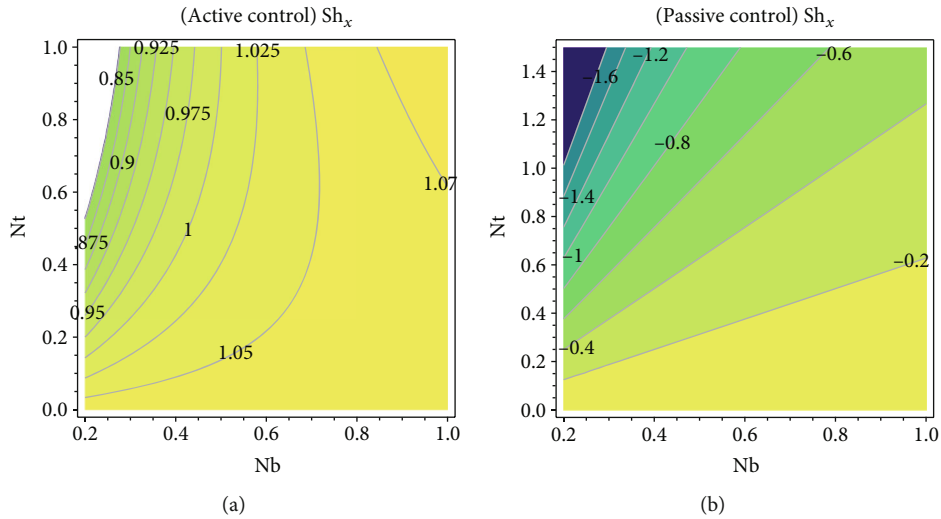


FIGURE 9: The effect of Sherwood number for combined parameters Nt and Nb .

the modified Hartmann number (Q) leads to producing a heat energy, and it is highly pronounced in the lesser value of modified Hartmann number Q , as seen in Figure 4(e).

Figure 5 illustrates the role of nanoparticle volume fraction on (a) thermophoresis parameter (Nt) and (b) Brownian motion parameter (Nb), for active and passive control cases. It is noted that for both behaviours of active and passive control, the Nb value increases. As we increase the Nb value, more resistive force is applied to the surface of the nanoparticle; thus, to increase the heat transfer, the nanoparticle volume fraction has to be increased. This increasing trend is reported in Figure 5(a) for both the cases of active and passive controls. As overturn to the above discussion, it is noted in Figure 5(b) that the volume fraction of nanoparticles decreases with an increase in the Brownian motion parameter, Nb . The fact is that the larger values of the Brownian motion parameter increase the length of the mean free path of the nanoparticle, which incredibly decreases the volume fraction of the nanoparticles.

The influence of the bioconvection Rayleigh number on the concentration of microorganisms is shown in Figure 6(a). With the increase in the Rayleigh number, the movement of microorganisms is increased; consequently, the concentration of microorganisms also increases. The role of the microorganism’s concentration difference parameter Ω in concentration is explored in Figure 6(b). For both the cases of active and passive controls, the trend is reported to be the same. In Figure 6(c), it is seen that the concentration of microorganisms increases as the bioconvection Lewis number Lb decreases. It is due to the variation in the temperature difference between the nanoparticles. It is noted in Figure 6(d) that the trend of active and passive control is in an opposite direction for the variation in the bioconvection Peclet number, Pe . As we increase the value of Pe , the diffusivity of microorganisms is decreased. Therefore, the concentration of microorganisms is decreased for passive control. Whereas the scenario is in active control, the trend is increased. The thermophoresis parameter Nt effect on

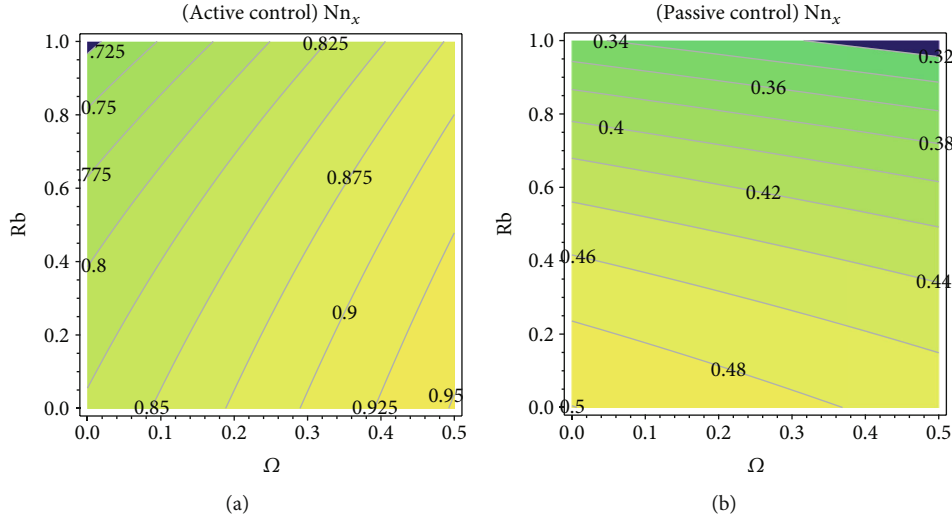


FIGURE 10: The effect of motile microorganism's density number for combined parameters Rb and Ω .

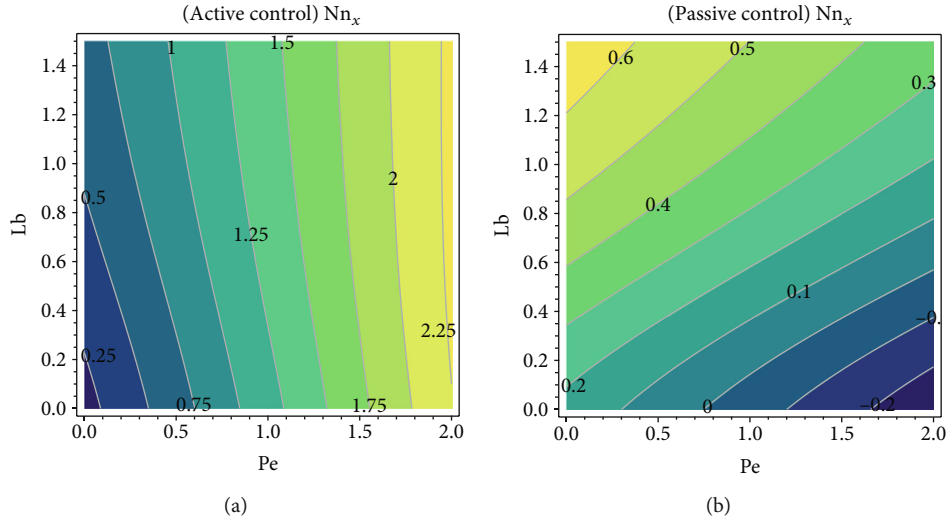


FIGURE 11: The effect of motile microorganism's density number for combined parameters Lb and Pe .

concentration of microorganisms is plotted in Figure 6(e). With the increase of Nt , the low heated nanoparticle is moved into the high heated surface which is induced by the increase in Nt . Hence, the concentration on microorganism is increased. In final, the variation in mixed convection parameter λ is analyzed in Figure 6(f). The increase in λ and the concentration on microorganisms is decreased. While for larger values of λ , temperature variation between the nanoparticles increases; therefore, this strongly affects the concentration of microorganisms.

Figures 7 and 8 depict the heat transfer rate (Nu_x) for different combinations of pertinent parameters. From Figure 7, the heat transfer rate enhances for higher values of modified Hartmann number (Q), and it decays for radiation parameter (Rd). Figure 8 elucidates that heat transfer rates reduce for larger values of γ and Hg . Figure 9 explores the combination of Nb and Nt in the mass transfer rate (Sh_x). It is noted from this figure that the mass transfer rate enhances for the Brownian motion parameter for active control while an opposite

behaviour is noticed for the thermophoresis parameter for both cases. Figures 10 and 11 portray the motile microorganism's density number rate (Nn_x) for different related parameters. From these figures, we found that the combined parameters Rb and Ω and Pe and Lb show the inverse effects on the microorganism's density number rate for active and passive controls.

6. Conclusion

In this work, the active and passive control of viscoelastic nanofluid flow over a 3D Riga plate is investigated analytically by the homotopy technique. Effects are studied with the influence of the gyrotactic microorganism in bioconvective heat transfer. The following outcomes are observed:

- (i) An increase in the modified Hartmann number produces the diminishing impact on velocity profile for both x and y directions

- (ii) Fluid velocity decays in both x and y directions for the augmentation in bioconvection Rayleigh number
- (iii) The microorganism profile is an increasing function of bioconvection Peclet number for active control, and it is decreasing for passive control
- (iv) Mass transfer rate enhances for Brownian motion parameter while an opposite behaviour is noticed for thermophoresis parameter for both cases
- (v) An increase in bioconvection Peclet number produces the inverse phenomena in microorganism profile for active and passive controls

Nomenclature

a, b :	Positive constants (-)
C :	Concentration (kgm^{-3})
C_{∞} :	Ambient concentration (kgm^{-3})
C_w :	Surface concentration of nanoparticles (kgm^{-3})
C_p :	Specific heat ($\text{J kg}^{-1} \text{K}^{-1}$)
C_{fx} :	Skin friction in x direction
C_{fy} :	Skin friction in y direction
d :	Chemotaxis constant (m)
D_B :	Brownian diffusion coefficient ($\text{m}^2 \text{s}^{-1}$)
D_T :	Thermophoretic diffusion coefficient ($\text{m}^2 \text{s}^{-1}$)
D_N :	Microorganism's diffusion coefficient ($\text{m}^2 \text{s}^{-1}$)
$f_1(\eta)$:	Velocity similarity function in x direction (-)
$g_1(\eta)$:	Velocity similarity function in y direction (-)
Hg:	Heat generation/absorption parameter (-)
k :	Thermal conductivity ($\text{m kg s}^{-3} \text{K}^{-1}$)
Le:	Lewis number (-)
L_b :	Bioconvection Lewis number (-)
Nb:	Brownian motion parameter (-)
Nt:	Thermophoresis parameter (-)
n_w :	Surface concentration of microorganisms (kgm^{-3})
n_{∞} :	Ambient concentration of microorganisms (kgm^{-3})
Nr:	Buoyancy ratio parameter (-)
Nu:	Nusselt number (-)
Nn:	Microorganisms' density number (-)
Pr:	Prandtl number (-)
P_e :	Bioconvection Peclet number (-)
Q :	Modified Hartmann number
Q_0 :	Dimensional heat generation/absorption coefficient
Rb:	Bioconvection Rayleigh number (-)
Rd:	Radiation parameter (-)
Sh:	Sherwood number (-)
T :	Temperature (K)
T_{∞} :	Ambient temperature (K)
u_w :	Velocity of the sheet (m s^{-1})
u, v, w :	Velocity components (m s^{-1})
W_c :	Maximum cell swimming speed (m s^{-1})
x, y, z :	Cartesian coordinates (m).

Greeks

α :	Material parameter of fluid
β :	Volume expansion coefficient (-)

γ :	Viscoelastic parameter (-)
$\phi_1(\eta)$:	Concentration similarity function (-)
ϵ :	Stretching ratio
η :	Similarity parameter (-)
$\xi_1(\eta)$:	Microorganisms' similarity function (-)
λ :	Mixed convection parameter (-)
ν :	Kinematic viscosity ($\text{m}^2 \text{s}^{-1}$)
τ :	Ratio of the effective heat capacity (-)
$\theta_1(\eta)$:	Temperature similarity function (-)
ρ :	Density (kgm^{-3})
ρ_f :	Density of nanofluid (kgm^{-3})
ρ_p :	Density of nanoparticles (kgm^{-3})
ρ_m :	Density of microorganism's particles (kgm^{-3})
σ :	Electrical conductivity ($\text{S}^3 \text{m}^2 \text{kg}^{-1}$)
ψ :	Stream function (ms^{-1})
Ω :	Microorganisms' concentration difference parameter (-).

Data Availability

The raw data supporting the conclusions of this article will be made available by the corresponding author without undue reservation.

Conflicts of Interest

The authors declare that they have no conflicts of interest.

Authors' Contributions

All authors listed have made a substantial, direct, and intellectual contribution to the work and approved it for publication.

References

- [1] T. J. Pedley and J. O. Kessler, "Hydrodynamic phenomena in suspensions of swimming microorganisms," *Annual Review of Fluid Mechanics*, vol. 24, no. 1, pp. 313–358, 1992.
- [2] K. Hosseinzadeh, S. Roghani, A. R. Mogharrebi, A. Asadi, M. Waqas, and D. D. Ganji, "Investigation of cross-fluid flow containing motile gyrotactic microorganisms and nanoparticles over a three-dimensional cylinder," *Alexandria Engineering Journal*, vol. 59, no. 5, pp. 3297–3307, 2020.
- [3] A. R. Mogharrebi, A. R. D. Ganji, K. Hosseinzadeh, S. Roghani, A. Asadi, and A. Fazlollahabbar, "Investigation of magnetohydrodynamic nanofluid flow contain motile oxytactic microorganisms over rotating cone," *International Journal of Numerical Methods for Heat & Fluid Flow*, 2021.
- [4] A. Ahmad, S. Asghar, and S. Afzal, "Flow of nanofluid past a Riga plate," *Journal of Magnetism and Magnetic Materials*, vol. 402, pp. 44–48, 2016.
- [5] R. Ahmad, M. Mustafa, and M. Turkyilmazoglu, "Buoyancy effects on nanofluid flow past a convectively heated vertical Riga- plate: a numerical study," *International Journal of Heat and Mass Transfer*, vol. 111, pp. 827–835, 2017.
- [6] N. Ahmed, Adnan, U. Khan, and S. T. Mohyud-Din, "Influence of thermal radiation and viscous dissipation on squeezed flow of water between Riga plates saturated with carbon

- nanotubes,” *Colloids and Surfaces A: Physicochemical and Engineering Aspects*, vol. 522, pp. 389–398, 2017.
- [7] A. Anjum, N. A. Mir, M. Farooq et al., “Physical aspects of heat generation/absorption in the second grade fluid flow due to Riga plate: application of Cattaneo-Christov approach,” *Results in Physics*, vol. 9, pp. 955–960, 2018.
- [8] A. Anjum, N. A. Mir, M. Farooq, M. I. Khan, and T. Hayat, “Influence of thermal stratification and slip conditions on stagnation point flow towards variable thicked Riga plate,” *Results in Physics*, vol. 9, pp. 1021–1030, 2018.
- [9] M. Farooq, A. Anjum, T. Hayat, and A. Alsaedi, “Melting heat transfer in the flow over a variable thicked Riga plate with homogeneous-heterogeneous reactions,” *Journal of Molecular Liquids*, vol. 224, pp. 1341–1347, 2016.
- [10] Y. Menni, A. J. Chamkha, M. Ghazvini et al., “Enhancement of the turbulent convective heat transfer in channels through the baffling technique and oil/multiwalled carbon nanotube nanofluids,” *Numerical Heat Transfer, Part A: Applications*, vol. 79, no. 4, pp. 311–351, 2021.
- [11] K. Loganathan, N. Alessa, K. Tamilvanan, and F. S. Alshammari, “Significances of Darcy–Forchheimer porous medium in third-grade nanofluid flow with entropy features,” *The European Physical Journal Special Topics*, 2021.
- [12] K. Loganathan, K. Mohana, M. Mohanraj, P. Sakthivel, and S. Rajan, “Impact of third-grade nanofluid flow across a convective surface in the presence of inclined Lorentz force: an approach to entropy optimization,” *Journal of Thermal Analysis and Calorimetry*, vol. 144, no. 5, pp. 1935–1947, 2021.
- [13] R. Maouedj, Y. Menni, M. Inc, Y. M. Chu, H. Ameer, and G. Lorenzini, “Simulating the turbulent hydrothermal behavior of oil/MWCNT nanofluid in a solar channel heat exchanger equipped with vortex generators,” *Computer Modeling in Engineering & Sciences*, vol. 126, no. 3, pp. 855–889, 2021.
- [14] A. Qayyum, T. Hayat, M. S. Alhuthali, and H. M. Malaikah, “Newtonian heating effects in three-dimensional flow of viscoelastic fluid,” *Chinese Physics B*, vol. 23, no. 5, p. 054703, 2014.
- [15] M. Shekholeslami, “New computational approach for exergy and entropy analysis of nanofluid under the impact of Lorentz force through a porous media,” *Computer Methods in Applied Mechanics and Engineering*, vol. 344, pp. 319–333, 2019.
- [16] M. Shekholeslami, A. N. Keshteli, and H. Babazadeh, “Nanoparticles favorable effects on performance of thermal storage units,” *Journal of Molecular Liquids*, vol. 300, p. 112329, 2020.
- [17] M. Shekholeslami, M. Jafaryar, A. Shafee, and H. Babazadeh, “Acceleration of discharge process of clean energy storage unit with insertion of porous foam considering nanoparticle enhanced paraffin,” *Journal of Cleaner Production*, vol. 261, p. 121206, 2020.
- [18] S. Khan, S. A. Shehzad, A. Rauf, and Z. Abbas, “Thermally developed unsteady viscoelastic micropolar nanofluid with modified heat/mass fluxes: a generalized model,” *Physica A: Statistical Mechanics and its Applications*, vol. 550, p. 123986, 2020.
- [19] M. Ahmad, T. Muhammad, I. Ahmad, and S. Aly, “Time-dependent 3D flow of viscoelastic nanofluid over an unsteady stretching surface,” *Physica A: Statistical Mechanics and its Applications*, vol. 551, p. 124004, 2020.
- [20] Z. Cao, J. Zhao, Z. Wang, F. Liu, and L. Zheng, “MHD flow and heat transfer of fractional Maxwell viscoelastic nanofluid over a moving plate,” *Journal of Molecular Liquids*, vol. 222, pp. 1121–1127, 2016.
- [21] M. Farooq, M. I. Khan, M. Waqas, T. Hayat, A. Alsaedi, and M. I. Khan, “MHD stagnation point flow of viscoelastic nanofluid with non-linear radiation effects,” *Journal of Molecular Liquids*, vol. 221, pp. 1097–1103, 2016.
- [22] T. Hayat, M. Sajid, and I. Pop, “Three-dimensional flow over a stretching surface in a viscoelastic fluid,” *Nonlinear Analysis: Real World Applications*, vol. 9, no. 4, pp. 1811–1822, 2008.
- [23] T. Hayat, T. Muhammad, A. Alsaedi, and M. S. Alhuthali, “Magnetohydrodynamic three-dimensional flow of viscoelastic nanofluid in the presence of nonlinear thermal radiation,” *Journal of Magnetism and Magnetic Materials*, vol. 385, pp. 222–229, 2015.
- [24] T. Hayat, F. Haider, T. Muhammad, and A. Alsaedi, “On Darcy-Forchheimer flow of viscoelastic nanofluids: a comparative study,” *Journal of Molecular Liquids*, vol. 233, pp. 278–287, 2017.
- [25] T. Hayat, S. Qayyum, S. A. Shehzad, and A. Alsaedi, “Cattaneo-Christov double-diffusion theory for three-dimensional flow of viscoelastic nanofluid with the effect of heat generation/absorption,” *Results in Physics*, vol. 8, pp. 489–495, 2018.
- [26] E. O. Alzahrani, Z. Shah, A. Dawar, and S. J. Malebary, “Hydromagnetic mixed convective third grade nanomaterial containing gyrotactic microorganisms toward a horizontal stretched surface,” *Alexandria Engineering Journal*, vol. 58, no. 4, pp. 1421–1429, 2019.
- [27] R. Naz, S. Tariq, and H. Alsulami, “Inquiry of entropy generation in stratified Walters' B nanofluid with swimming gyrotactic microorganisms,” *Alexandria Engineering Journal*, vol. 59, no. 1, pp. 247–261, 2020.
- [28] N. Acharya, K. Das, and P. K. Kundu, “Framing the effects of solar radiation on magneto-hydrodynamics bioconvection nanofluid flow in presence of gyrotactic microorganisms,” *Journal of Molecular Liquids*, vol. 222, pp. 28–37, 2016.
- [29] W. Khan and O. D. Makinde, “MHD nanofluid bioconvection due to gyrotactic microorganisms over a convectively heat stretching sheet,” *International Journal of Thermal Sciences*, vol. 81, pp. 118–124, 2014.
- [30] M. Ijaz Khan, M. Waqas, T. Hayat, M. Imran Khan, and A. Alsaedi, “Behavior of stratification phenomenon in flow of Maxwell nanomaterial with motile gyrotactic microorganisms in the presence of magnetic field,” *International Journal of Mechanical Sciences*, vol. 131–132, pp. 426–434, 2017.
- [31] H. Waqas, S. U. Khan, M. Hassan, M. M. Bhatti, and M. Imran, “Analysis on the bioconvection flow of modified second-grade nanofluid containing gyrotactic microorganisms and nanoparticles,” *Journal of Molecular Liquids*, vol. 291, p. 111231, 2019.
- [32] M. T. Sk, K. Das, and P. K. Kundu, “Multiple slip effects on bioconvection of nanofluid flow containing gyrotactic microorganisms and nanoparticles,” *Journal of Molecular Liquids*, vol. 220, pp. 518–526, 2016.
- [33] E. Elanchezhian, R. Nirmalkumar, M. Balamurugan, K. Mohana, K. M. Prabu, and A. Vilorio, “Heat and mass transmission of an Oldroyd-B nanofluid flow through a stratified medium with swimming of motile gyrotactic microorganisms and nanoparticles,” *Journal of Thermal Analysis and Calorimetry*, vol. 141, no. 6, pp. 2613–2623, 2020.
- [34] K. Hosseinzadeh, S. Roghani, A. R. Mogharrebi, A. Asadi, and D. D. Ganji, “Optimization of hybrid nanoparticles with mixture fluid flow in an octagonal porous medium by effect of radiation and magnetic field,” *Journal of Thermal Analysis and Calorimetry*, vol. 143, no. 2, pp. 1413–1424, 2021.

- [35] M. Ijaz Khan, F. Haq, S. A. Khan, T. Hayat, and M. Imran Khan, "Development of thixotropic nanomaterial in fluid flow with gyrotactic microorganisms, activation energy, mixed convection," *Computer Methods and Programs in Biomedicine*, vol. 187, p. 105186, 2020.
- [36] G. K. Ramesh, "Analysis of active and passive control of nanoparticles in viscoelastic nanomaterial inspired by activation energy and chemical reaction," *Physica A: Statistical Mechanics and its Applications*, vol. 550, p. 123964, 2020.
- [37] N. Acharya, K. Das, and P. Kumar Kundu, "Fabrication of active and passive controls of nanoparticles of unsteady nanofluid flow from a spinning body using HPM," *The European Physical Journal Plus*, vol. 132, no. 7, p. 323, 2017.
- [38] N. Acharya, "Active-passive controls of liquid di-hydrogen mono-oxide based nanofluidic transport over a bended surface," *International Journal of Hydrogen Energy*, vol. 44, no. 50, pp. 27600–27614, 2019.
- [39] S. S. Giri, K. Das, and P. K. Kundu, "Stefan blowing effects on MHD bioconvection flow of a nanofluid in the presence of gyrotactic microorganisms with active and passive nanoparticles flux," *The European Physical Journal Plus*, vol. 132, no. 2, 2017.
- [40] T. Hayat, A. Aziz, T. Muhammad, and A. Alsaedi, "Active and passive controls of Jeffrey nanofluid flow over a nonlinear stretching surface," *Results in Physics*, vol. 7, pp. 4071–4078, 2017.
- [41] J. Jiang and X. Yu, "Fault-tolerant control systems: a comparative study between active and passive approaches," *Annual Reviews in Control*, vol. 36, no. 1, pp. 60–72, 2012.
- [42] S. Eswaramoorthi and M. Bhuvanewari, "Passive and active control on 3D convective flow of viscoelastic nanofluid with heat generation and convective heating," *Frontiers of Mechanical Engineering*, vol. 5, 2019.
- [43] R. Tripathi, G. S. Seth, and M. K. Mishra, "Double diffusive flow of a hydromagnetic nanofluid in a rotating channel with Hall effect and viscous dissipation: active and passive control of nanoparticles," *Powder Technology*, vol. 28, no. 10, pp. 2630–2641, 2017.
- [44] N. Wang, A. Maleki, M. Alhuyi Nazari, I. Tlili, and M. Safdari Shadloo, "Thermal conductivity modeling of nanofluids contain MgO particles by employing different approaches," *Symmetry*, vol. 12, no. 2, p. 206, 2020.
- [45] S. Liao and Y. A. Tan, "A general approach to obtain series solutions of nonlinear differential equations," *Studies in Applied Mathematics*, vol. 119, no. 4, pp. 297–354, 2007.
- [46] K. Loganathan and S. Rajan, "An entropy approach of Williamson nanofluid flow with joule heating and zero nanoparticle mass flux," *Journal of Thermal Analysis and Calorimetry*, vol. 141, no. 6, pp. 2599–2612, 2020.
- [47] N. Freidoonimehr and A. B. Rahimi, "Brownian motion effect on heat transfer of a three-dimensional nanofluid flow over a stretched sheet with velocity slip," *Journal of Thermal Analysis and Calorimetry*, vol. 135, no. 1, pp. 207–222, 2019.
- [48] K. Loganathan, S. Sivasankaran, M. Bhuvanewari, and S. Rajan, "Second-order slip, cross-diffusion and chemical reaction effects on magneto-convection of Oldroyd-B liquid using Cattaneo–Christov heat flux with convective heating," *Journal of Thermal Analysis and Calorimetry*, vol. 136, no. 1, pp. 401–409, 2019.
- [49] T. Hayat, M. Ijaz Khan, S. Qayyum, and A. Alsaedi, "Modern developments about statistical declaration and probable error for skin friction and Nusselt number with copper and silver nanoparticles," *Chinese Journal of Physics*, vol. 55, no. 6, pp. 2501–2513, 2017.
- [50] M. Farooq, M. Javed, M. Ijaz Khan, A. Anjum, and T. Hayat, "Melting heat transfer and double stratification in stagnation flow of viscous nanofluid," *Results in Physics*, vol. 7, pp. 2296–2301, 2017.
- [51] K. Loganathan, G. Muhiuddin, A. M. Alanazi, F. S. Alshammari, B. M. Alqurashi, and S. Rajan, "Entropy optimization of third-grade nanofluid slip flow embedded in a porous sheet with zero mass flux and a non-Fourier heat flux model," *Frontiers of Physics*, vol. 8, p. 250, 2020.